Investigation of the ballistic performance of Ultra High Molecular Weight Polyethylene composite panels

Tomasz K. Ćwik[☆a], Lorenzo Iannucci[a], Paul Curtis[a,b], Dan Pope[b]

[a] *Department of Aeronautics, Imperial College of Science and Technology, London, UK*
[b] *DSTL, Porton Down, UK*

Abstract

The ballistic performance of Dyneema® HB26 and Spectra® 3124 subjected to high velocity impact of steel and copper Fragment Simulating Projectiles was evaluated. A 3D High Speed Digital Image Correlation was used for measurement of the panels front face deformation and the back face deformation. The information obtained from the measurements, along with the post-mortem observation of the panels, allowed to draw conclusions with respect to the importance of various energy dissipation mechanisms that occurred in the tested materials. It was observed that, although Dyneema® HB26 and Spectra® 3124 deform very differently during the impact event, they had a similar ballistic performance.

Keywords: Dyneema, Spectra, UHMWPE, ballistics, impact

1. Introduction

High performance composite materials are currently extensively used in various defence applications requiring high protection levels and low weight at the same time. Typically, unidirectional (UD) cross ply (X-ply) laminates provide better protection against ballistic threats than composites reinforced with woven fabrics, whereas the latter tend to provide better protection than the UD X-ply laminates when exposed to blast threats. An extensive overview of ballistic studies on fabrics and compliant composite laminates was provided by Cheeseman & Bogetti [1]. The authors noted the importance of material properties and the fabric structure when designing against impact. The influence of the projectile geometry and the striking velocity, as well as many other factors, on the ballistic response of various materials were also discussed. Although a number of publications contributed to increasing the understanding of dynamic behaviour of compliant laminates, the processes occurring in these composites during impacts are still not fully understood. Iremonger & Went [2] conducted ballistic trials on Nylon 6.6/EVA laminates subjected to impact from a 1.1 gram Fragment Simulating Projectile (FSP). The authors noted that the fibres located in front face of the panel experienced one of the two different failure modes (transverse shear of fibres or stretch and tensile failure of fibres) depending on which edge of the projectile they were in contact. Prosser [3] investigated ballistic performance of a multilayer Nylon 6,6 fabric impacted with 0.22 FSPs. The author identified that the work of penetration per interior layer was constant. Penetration mechanisms were described in part II of his work [4], which is focused on providing more evidence that the major mode of failure of the Nylon panels impacted by the FSP were cutting and shearing mechanisms. Ballistic performance of Nylon 6,6 was also compared with the performance of Kevlar 29 in Figucia et al. [5]. The authors observed that tensile yarn straining was the main energy dissipating mechanisms in the tested fabrics, while the strain wave velocity was concluded to be the most influential parameter affecting the ballistic performance of the materials. An investigation of the ballistic performance of composites reinforced with aramid and ultra high molecular weight polyethylene (UHMWPE) fibres was conducted by Scott [6]. The author compared deformation characteristics, caused by the projectile impact, of rigid and compliant laminates. Similarly to

☆Corresponding author
Email address: tomasz.cwik@imperial.ac.uk (Tomasz K. Ćwik☆)

observations made by Iremonger [2], Scott highlighted the fact that there was a spring-back effect in the compliant laminates i.e. the fibres at the front face after being compressed by the projectile, and having fractured, spring back in the direction opposite to the projectile flight. Lee et al. [7] noted in their ballistic study involving Spectra 900® that although the matrix system did not seem to absorb substantial amounts of the impact energy, it definitely contributed to the overall amount of the energy absorbed by the composite. Flanagan et al. [8] compared ballistic performance of various fabrics of different architectures, made of Spectra 1000®, Kevlar 129®, and Twaron 2000®. An epoxy resin was used as the matrix system. 12 gram right cylinder projectiles with a length-to-diameter ratio of 3 were fired at 200 - 1100 m/s. It was observed that the failure modes experienced by the panels changed with increasing the striking velocity. At velocities higher than 800 m/s shear-plug formation was the main failure mode at the front face of the panels, whereas fibre breakage and pullout were observed at the back face of the panels. Cunniff [9] showed that the ballistic performance of composites reinforced with highly aligned polymeric fibres (e.g. Dyneema®, Kevlar®, Spectra®, Zylon® etc.) depends largely on the yarns sonic velocity and the energy-based mass absorption capacity of the fibres . Although the dimensionless analysis proposed by Cunniff provides reasonable predictions for some materials made of the high performance fibres, it is a "first-level screening tool to assess the performance of fibres" as noted by Cheeseman & Bogetti [1]. The analysis simplifies the impact problem to only two parameters which are related to the yarn physical and mechanical properties. The analysis does not take into consideration: strain rate effects in the fibres, non-linearity of the yarn stress-strain curve, plastic deformation of the yarns, influence of the composite matrix system and all the associated phenomena.

This paper presents results of ballistic testing of Dyneema® HB26 and Spectra® 3124. Dyneema® HB26 is a product made by DSM Dyneema, whereas Spectra 3124 is produced by Honeywell. The tests were conducted to provide validation data for high fidelity numerical codes. A highly instrumented experimental setup was used to obtain qualitative information regarding deformation and strain distributions on both the front and rear faces of the panel during the impact event. The high quality impact data provide an insight into understanding the physical phenomena taking place in these two high performance composite materials during projectile penetration, and thus identify to what extent the ballistic properties of the panels are actually dependant on the properties of the expensive high performance fibres. The information should help improve numerical modelling techniques and analytical methods used to determine the V_{50} of a laminate.

2. Materials

The following materials were tested in this study: Dyneema® HB26, Spectra® 3124. Both had a 0/90 cross ply layup and were provided as already consolidated panels. All tested panels had areal density of 23.5 kg/m^2 and were 300 x 300 mm. The nominal thickness of all panels was 23 mm, however the average measured thicknesses were 24.02 mm and 24.08 mm for the Dyneema® and the Spectra®, respectively. According to the authors best knowledge, areal density of single ply of Dyneema® and Spectra® were similar and close to 260 g/m^2 i.e. both type of panels had about 90 plies. The average weight of the panels was 2.118 kg and 2.060 kg for Dyneema® and Spectra®, respectively. 15 Dyneema® panels and 12 Spectra® panels were tested.

3. Experimental setup

The trials employed 20 mm diameter steel and copper Fragment Simulating Projectiles (FSPs) fired at up to 1.2 km/s at zero obliquity by a powder gas gun. The steel projectiles were manufactured to STANAG 2920 [10], while the copper projectiles had exactly the same geometry, but higher mass (as a consequence of the density of copper). A standard copper was used for the projectiles (ρ= 8930 kg/m^3, E= 110 GPa, σ_Y= 70 MPa). The projectiles weighed 53.1±0.15 gram and 60.25±0.25 gram, respectively.

The back face of the tested plates was supported in all four edges. The panels were clamped by four clamps with bolts fastened in the direction transverse to the flight of the projectile, as shown in Figure 1 (the panel is shown in orange). This clamping system guaranteed the panel remained in place, while no substantial compression force was applied to the panel. No holes were made in the panels. Most of the figures in this paper showing snapshots from high speed videos show the entire width of the panel visible from the back of the rig, i.e. 250 mm in Figure 1, and slightly more than half of the panel hight i.e. about 150 mm.

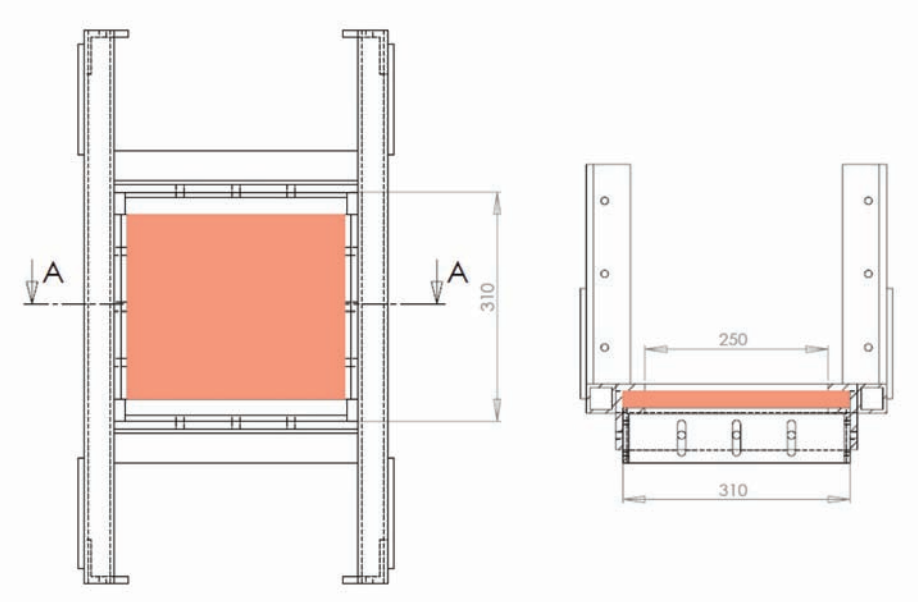

Figure 1: The CAD drawing of the ballistic rig used in the study.

A typical experimental setup is presented in the Figure 2 (schematically) and Figure 3 (in practice). Up to six Vision Research high speed cameras were used during the trials. Table 1 lists all the high speed cameras used for the study and their settings. All cameras had a common trigger and common time reference (IRIG). This allowed to correlate the recorded deformation observed at the front face with the back face deformation. Additionally, the cameras used for the DIC had their frames synchronized (F-sync). The striking velocity of the projectile was measured either by an infrared gate or by Doppler radar. Typically, two high speed cameras were used for the front face 3D Digital Image Correlation (DIC), another two cameras were used for the rear face 3D DIC, and one high speed camera was used for measurement of the residual velocity. When the front face 3D DIC set was unavailable, a single high speed camera was used for recording the front face deformation. The rear DIC cameras were positioned approximately 1.6 m away from the target, whereas the front DIC cameras were approximately 1.5 m from the target. Projectiles which penetrated panels were caught in a wooden catcher box filled with sand and rags.

A C-shape object, shown in Figure 3b, of known dimensions was used as the calibration object for the residual velocity camera. The software used for the high speed cameras has an inbuilt algorithm for measurement of displacement and velocity of the observed object, but it requires defining a known reference length. In this case, the length was defined by using the C-shape object. Tracing paper was used to dim the light required for illumination of silhouette of the projectile and panel observed by the residual velocity camera.

The speckle pattern was painted on the panels and on the test rig using black markers. The dots on the rig were made in order to identify whether the rig moved during the experiments. It was found that the movement of the rig during the experiments was negligible and therefore it was not necessary to subtract it from the movement/deformation of the panel.

4. Results and discussion

4.1. Ballistic curves

Greenhalgh at al. [11] postulates that different processing conditions (consolidation pressure during fabrication) may influence the global failure mechanism characteristics occurring in consolidated polyethylene panels, subjected to impact loading. As a result the panels may have different ballistic performance depending on the manufacturing cycle adopted and whether it was optimised for ballistic impact. The Dyneema® panels used in this study were provided by DSM, but the processing cycle was not disclosed to the authors. Similarly, the processing cycle

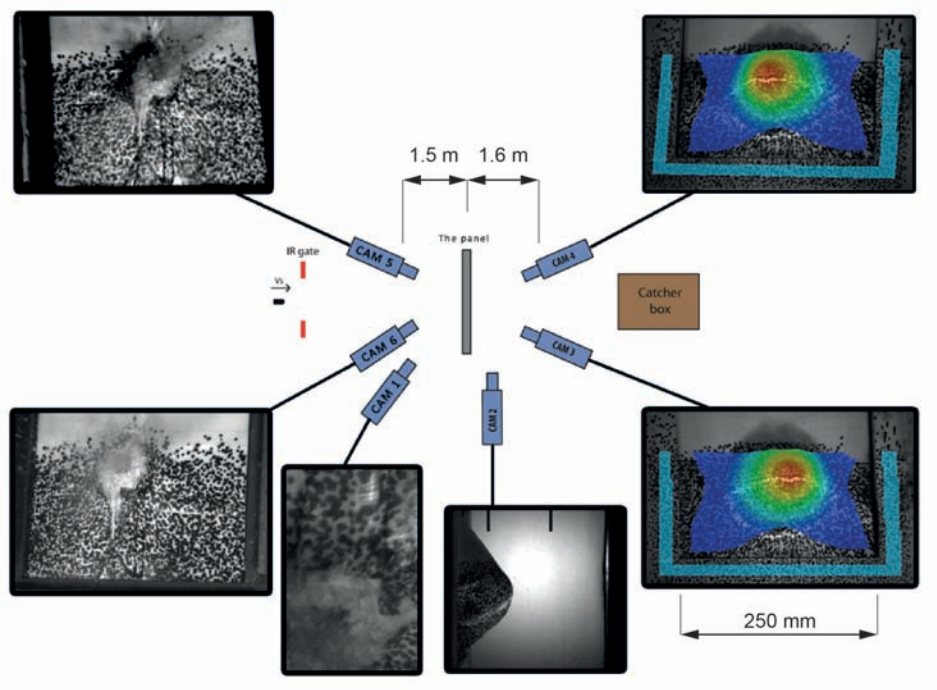

Figure 2: Schematic diagram of the experimental setup.

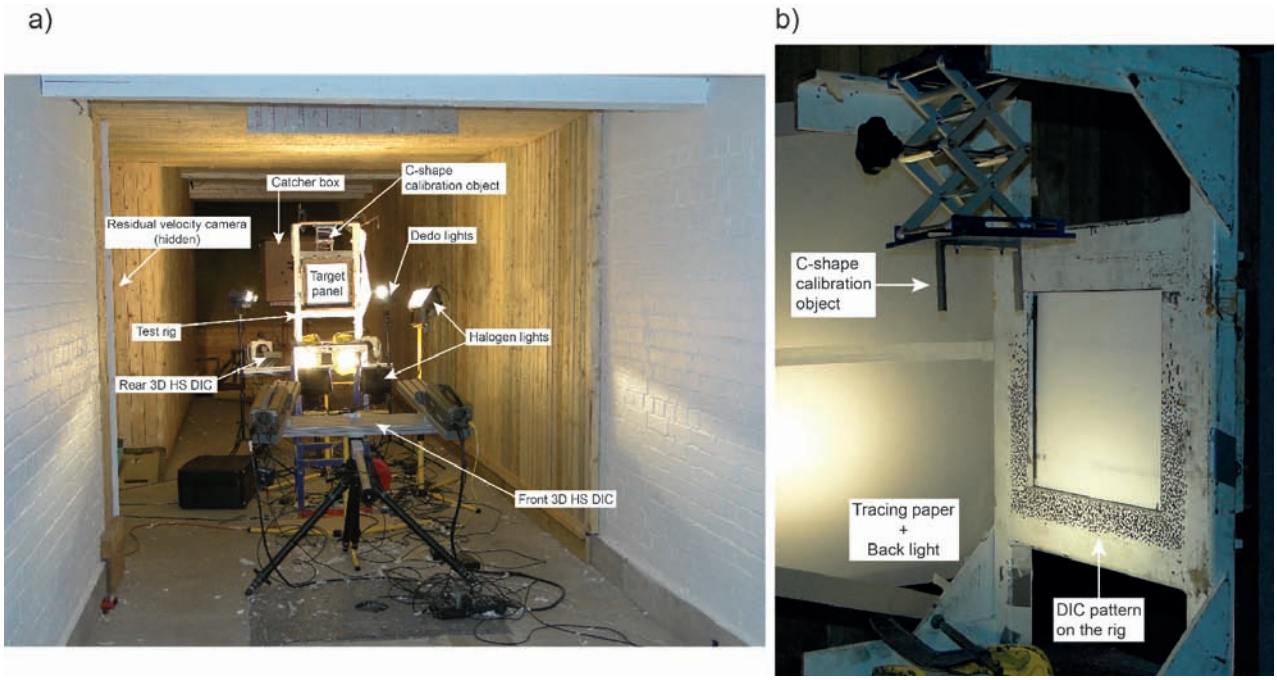

Figure 3: The actual ballistic testing experimental setup.

Table 1: Specification of the Phantom cameras setup used in this study.

	Dyneema® HB26	**Spectra® 3124**
Front 3D HS DIC set		
Camera model	-	Phantom V711
Frame rate	-	39k fps
Resolution	-	464 x 320 px
Lens	-	50mm Nikon
Rear 3D HS DIC set		
Camera model	Phantom V711	Phantom V16
Frame rate	41k fps	82k fps
Resolution	512 x 304 px	512 x 304 px
Lens	50mm Nikon	50mm Nikon
Side camera		
Camera model	Phantom V16	Phantom V12
Frame rate	87k fps	62k fps
Resolution	284 x 336 px	256 x 280 px
Lens	100mm Carl Zeiss	24-85mm Nikon
Front camera		
Camera model	Phantom V12	Phantom V12
Frame rate	21k fps	65k fps
Resolution	512 x 512 px	200 x 304 px
Lens	50mm Nikon	100mm Carl Zeiss

of Spectra® remains unknown to the authors as the panels were provided by a third-party supplier who manufactured them using the standard recommended cycle. Therefore, it should be noted that the ballistic behaviour of the two materials may have been influenced by the manufacturing processes used to make them.

The ballistic trials were conducted in a slightly different manner than a conventional V_{50} trial. Due to the fact the aim of the trials was to generate large amounts of data required for validation of advanced numerical simulations (i.e. the estimation of V_{50} was not the main goal) and because a limited number of panels were available for the study, the striking velocity, Vs, was increased every shot by approximately 100 m/s up to more than 1 km/s. Figure 4 presents the ballistic curves. *St* denotes Steel, while *Cu* denotes Copper. During the trials it was observed that in some tests the rear part of the panel debonded and flew off with the projectile i.e. the projectile was not visible to the cameras. In these cases the residual velocity was measured from the movement of the panel (not the projectile) and these shots are denoted "BF" in Figure 4, which stands for "Back Face" measurement. These residual velocity values should be treated with caution, as clearly if the panel was larger additional work would be performed in failing the ejected composite.

The collected data indicated that the ballistic limit (BL) of the materials is approximately in the region of: 700 m/s for Dyneema® HB26 impacted with steel and copper FSPs; and 600 m/s for Spectra® 3124 impacted with steel, while approximately 700 m/s when impacted with copper FSPs. The data is not sufficient to provide more precise estimates of the ballistic limits. It should be also emphasized, once again, that the edge effects might have influenced the response of the panels. In the firings in which the residual velocity was measured from the panels' back face, most likely the projectile would be caught, if a larger panel was used. Thus, the ballistic limits could have been different.

4.2. Deformation of the projectiles

The projectiles which penetrated the panels were caught by the catcher box filled with sand and rags. Prior to the experiments test projectiles were shot into the catcher box, with no panel in the ballistic rig, to identify the influence of the box and the sand on the deformation of the projectile. It was found that the steel projectiles did not deform, irrespectively of the striking velocity. The copper projectiles fired at low velocities (e.g. 200-400 m/s) did not deform during the catching process. However, copper projectiles fired at high velocities (e.g. 1 km/s) deformed to a certain extent. Figure 5a shows a copper projectile that was fired at 1 km/s into the catcher box. It was observed that the projectile deformed due to the impact. Therefore, the deformation of the projectiles presented in the Figure 5d and

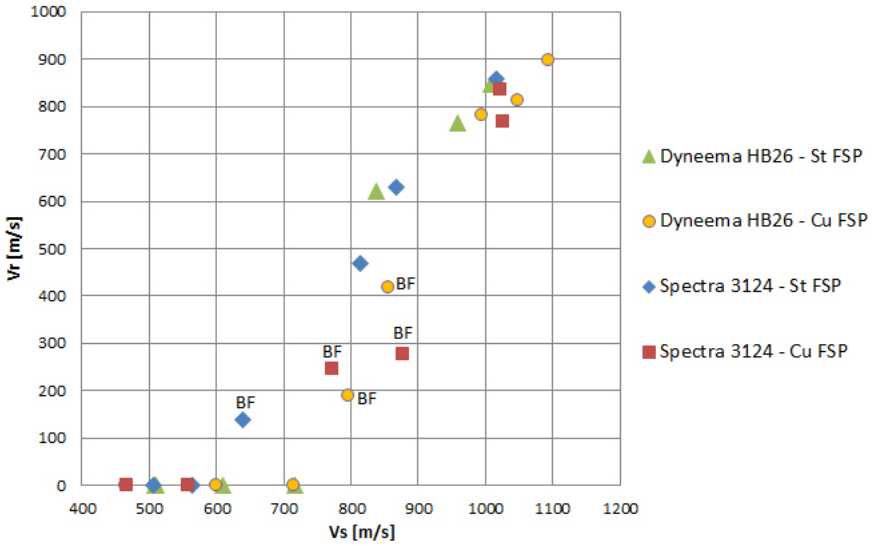

Figure 4: Experimental points for Dyneema® HB26 and Spectra® 3124, for copper and steel FSPs.

e is a resultant of the deformation during penetration of the tested panel and during the penetration of the catcher box.

No weight loss of the steel projectiles was noticed for all tests. The copper projectiles deformed substantially during the impact, however any significant weight loss was only noticed for two projectiles which impacted Dyneema® panels at 1047 m/s and 1094 m/s (the two projectiles lost 1.49g and 2.58g of mass, respectively). The extent of deformation of the copper FSPs increased along with the increasing striking velocity.

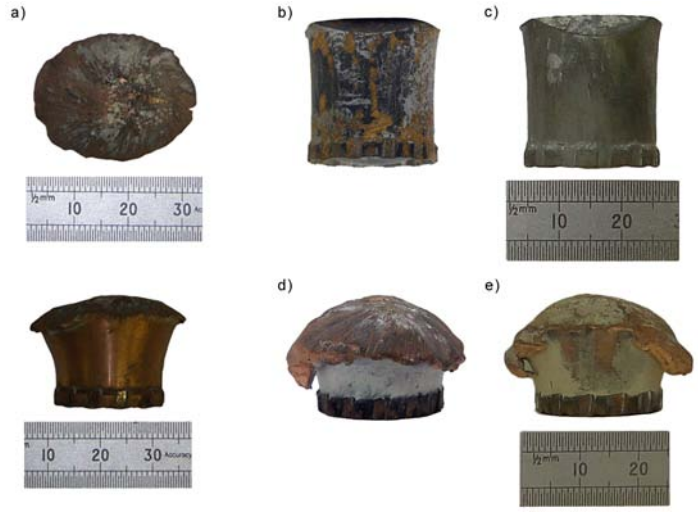

Figure 5: Photographs of the post-mortem projectiles: a) The copper FSP fired into the catcher box at 1 km/s (top view and side view); b) St FSP, Dyneema® HB26, Vs=1008 m/s; c) St FSP, Spectra® 3124, Vs=1016 m/s; d) Cu FSP, Dyneema® HB26, Vs=1047 m/s; e) Cu FSP, Spectra® 3124, Vs=1027 m/s.

The data in Table 2 indicates that panels impacted with copper projectiles lost more weight than panels impacted with steel projectiles. Dyneema® and Spectra® panels lost on average 0.129% and 0.048% of their initial weight, respectively, when impacted with steel projectiles; while 0.271% and 0.048% average weight loss was observed for the two materials respectively, when impacted with a copper projectile. This is probably the result of copper low yield strength (and possibly due to the shock heating discussed in the next section) which allowed for more extensive

plastic deformation of the projectile during the impact event, as it was shown in Figure 5. The "mushroomed" copper projectile has a greater effective area which allows it to affect (e.g. tear or melt) a larger amount of the material that is in contact. The data for copper projectiles shows also that the weight loss is greater for shots above the BL. In terms of the steel projectiles, it is difficult to say whether more material was lost with shots fired above the BL velocity, as the measured difference of the lost mass was very small and the number of tested panels was not sufficient to observe any trends.

Table 2: The average panel weight loss after the impact.

	Units	Dyneema® HB26		Spectra® 3124	
FSP type		St	Cu	St	Cu
Below BL	g	3.5	4.5	1.0	0
Above BL	g	2.0	7.0	1.0	2.0

4.3. The front face deformation

It is known that a material is in the hydrodynamic state if the velocity of the waves propagating in the material is higher than the sound velocity in the material i.e. there is a shock wave in the material. Figure 6 shows the Equation of State (EoS) curves for Dyneema® (in-fibre direction - the red dots; and in transverse direction - blue dots), as well as for bulk polyethylene (PE), coming from reference [12] in which the authors reference results from other studies (i.e. the PE results). The figure shows that the sound velocity in the transverse direction of Dyneema® is slightly less than 2 km/s. If the material is impacted at the particle velocity (i.e. the striking velocity) of 400 m/s or higher, a shock is created in the material which propagates at a velocity higher than the sound velocity in the transverse direction of Dyneema®. Considering the fact that similar striking velocities were used in the presented study, it is fair to presume that a certain region of the Dyneema® panel was in the hydrodynamic state during the ballistic test. Due

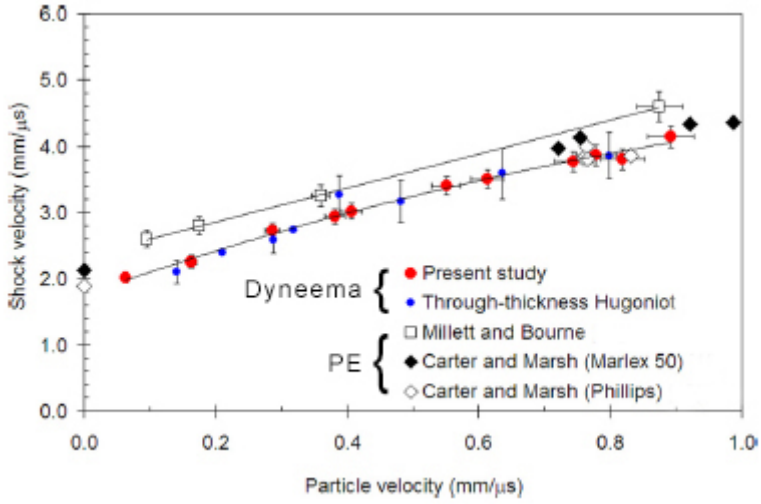

Figure 6: The EoS curves for Dyneema® and PE [12].

to the additional high speed camera that was recording the very point of impact every 15.38 μs, during the trials with Spectra® 3124, it was possible to observe that actually during the first 15.38 μs, although the projectile was penetrating the panel, there was no lateral movement of the adjacent material at all. Any movement of the material was observed in the subsequent frames (30.76μs and later). This indicates that for at least the first 15.38 μs, but less than 30.76 μs, a certain part of the front face material experienced an inelastic deformation. Figure 7 presents snapshots from the Phantom camera. Assuming that the Equation of State (EoS) of Spectra 3124® is similar to the Dyneema® EoS (as both composites have the same mass density and they consist of similar polyethylene fibres) considering the observations

from the high speed videos, it is very likely that certain regions of the Spectra® panel were also in the hydrodynamic state during the conducted experiments.

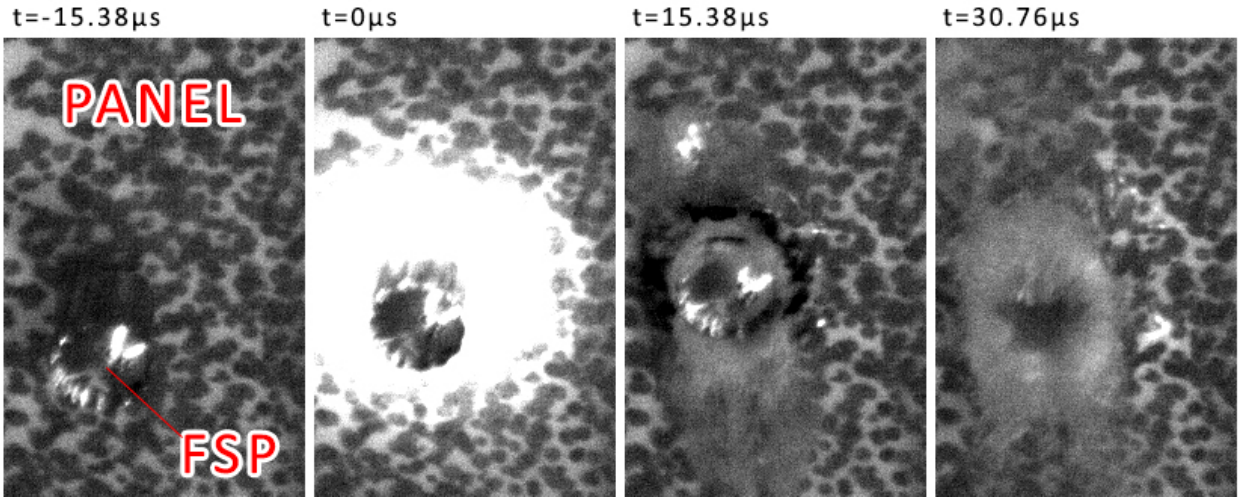

Figure 7: Front face, magnified view of Spectra® 3124 panel impacted with copper FSP at 773 m/s.

It was observed that during all experiments at the instance of projectile-panel contact a bright flash, circular in shape was generated (see Figure 8). The shape of the flash changed from the circle to a peanut as the projectile started penetrating the panel. This was followed by ejection of fragmented stoke melted material from the sides of the projectile chiselled nose, and then by a global deformation of the front face and ejection of larger quantities of the material. It was not identified whether the ejecta consisted of the polyurethane (PU) resin, or the polyethylene fibres, or both. It is believed that the flash was a result of the pressure rise at the projectile-panel interface and in the adjacent

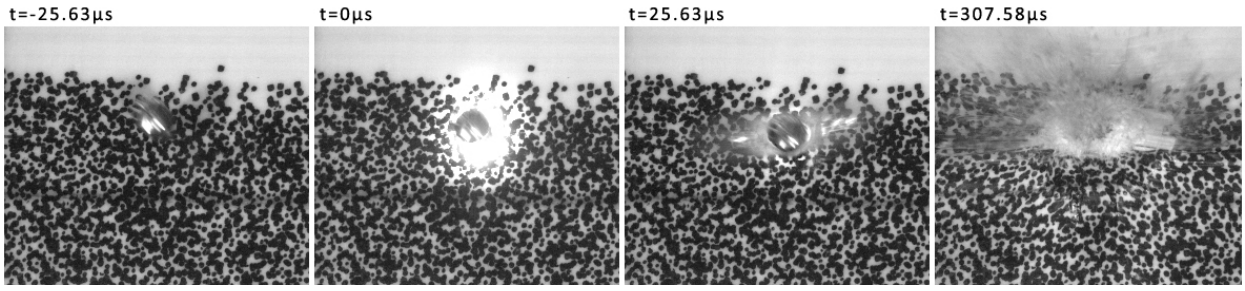

Figure 8: Front face view of a Spectra® 3124 panel impacted with copper FSP at 773 m/s.

areas due to shock loading induced by the impacting projectile, which caused the rise of the temperature in both bodies. Figure 9 and Figure 10 present how the temperature and pressure changes in Dyneema® during shock loading, with respect to the striking velocity, respectively. The charts were created based on the data from reference [12]. Following Hazel et al. [12], the temperature during shock loading was approximated by calculating the temperature along the adiabat (T_a) using the following equation:

$$T_a = T_1 exp[\Gamma - \Gamma(\frac{v}{v_0})] \tag{1}$$

The pressure in the material was calculated as follows:

$$p = \rho U_s u_p \tag{2}$$

where Γ is Gruneisen gamma, T_1 is the initial temperature of the sample (300^{o}K), v_0 is the specific volume at ambient conditions, ρ is the mass density of the material, U_s is the shock velocity, and u_p is the particle velocity (i.e. the striking velocity). The Equation of State (EoS) of Dyneema® in the through thickness direction was given by $U_s = 1.81 + 2.72U_p$ based on the information provided by Hazel et al. [12]. Additionally, the charts contain information about the melting temperature of the Dyneema® fibres, denoted as "PE" in the charts, and about the thermoplastic polyurethane (TPU) resin. The melting temperature range of the former is 144-152^{o}C [13], whereas the TPU resin melts at about 180^{o}C [14]. Figure 9 shows that below the striking velocity of 800 m/s, neither PE fibres nor TPU

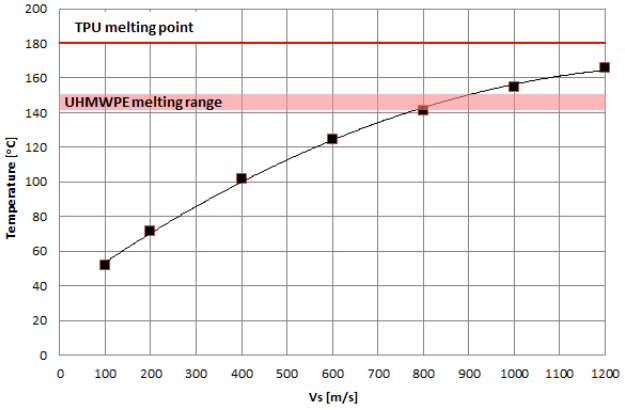

Figure 9: Temperature rise along the adiabat for compressed Dyneema®.

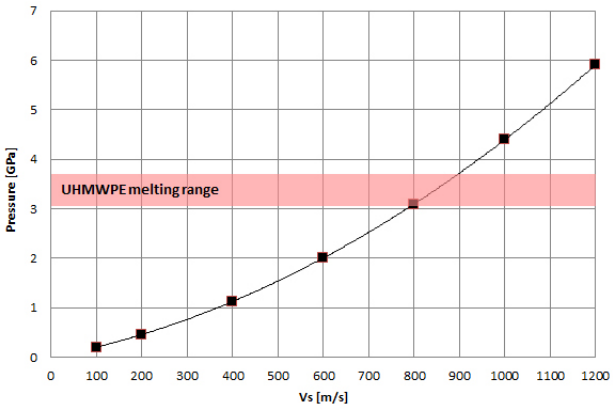

Figure 10: Pressure rise in the compressed Dyneema®.

melts. At striking velocities higher than 800 m/s only the PE fibres melts. The latter would explain why both Spectra 3124® and Dyneema HB26® tested in this study had very similar residual velocities for the striking velocities higher than 850 m/s (see Figure 4). Figure 7 in Hazel et al. [12] shows that no melting was observed at striking velocities of 259 m/s and 600 m/s, however melting was observed in the material impacted at 947 m/s. Greenhalgh et al. [11], however, conducted a fractographic analysis of similarly tested panels and concluded that the matrix resin melted and resolidified on the fibres after the impact. Thus, a more detailed fractographic analysis of the panels tested in this study would identify what actually melted.

Figure 11 and Figure 12 present out-of-plane and in-plane displacement of a point selected on the surface of three Spectra® panels, for the two projectile types, obtained from the front face 3D High Speed DIC. It should be emphasized that the measured points were not exactly the very same points in each case. Also, due to the destructive nature of the experiment it was impossible to obtain any DIC readings from the very impact point. As a result, the points as close to the impact point as possible were selected. Typically the measurement point was 50 mm below the impact point, in the horizontal centre of the panel. The DIC measurements show that the in-plane movement of the material occurred first, before the out-of-plane movement. The former started approximately after the first 50 μs of the projectile penetration, while the latter approximately after 100 μs. This is no surprise as the sonic velocity along the Dyneema® fibres is much higher than the transverse velocity through the Dyneema® panel. Figure 12 shows that the projectile material did not influence the in-plane response of the front part of the Spectra® panels, during the initial stages of the impact. However, it was observed that the velocity of the deformation depends on the striking velocity (the slope of the curves is higher for impacts at lower striking velocities). The panels impacted at lower velocities tended to deform in-plane quicker than the panels impacted at higher velocities. In terms of the out-of-plane panel displacement, it was observed that the projectile material influenced the response of the panel. Panels impacted with copper FSPs deformed more than the ones impacted with steel FSPs. Figure 13 and Figure 14 show the front face of an impacted Dyneema panel and a cross section view at the impact area, respectively. The compression deformation observed around the impact hole in Figure 13 (but also present in many other tested panels), that resembles a typical open hole problem, occurred at the later stages of deformation, long after the projectile penetrated the initial thickness of the panel. The deformation was onset by the moving projectile which pushed away the adjacent material, as showed in the Figure 7, at about 31 μs after the impact. From then on, the wrinkles propagated towards the edges of the panel, resulting in the type of deformation observed in the Figure 13.

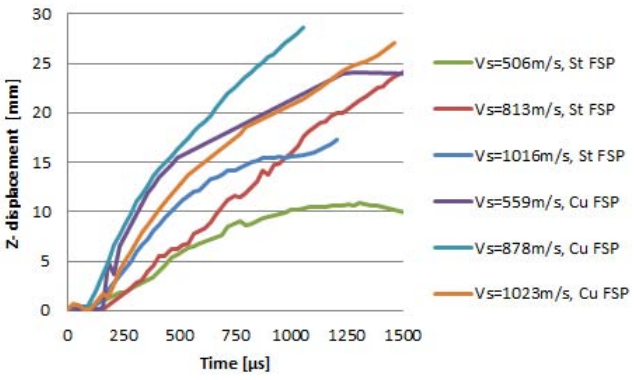

Figure 11: The out-of-plane time-displacement history of a point on the front surface of Spectra® 3124.

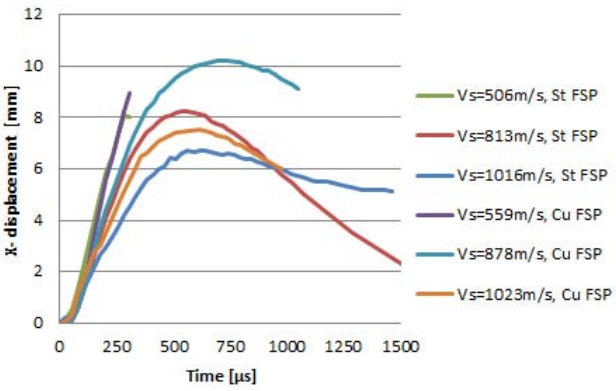

Figure 12: The in-plane time-displacement (in horizontal direction) history of a point on the front surface of Spectra® 3124.

The DIC measurements showed that the Spectra® front face experiences less than 1% tensile strain during the

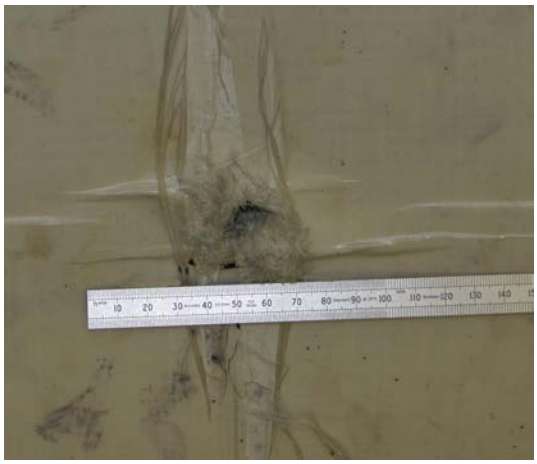

Figure 13: Magnified view on the Dyneema® HB26 panel impacted at 509 m/s by a steel FSP.

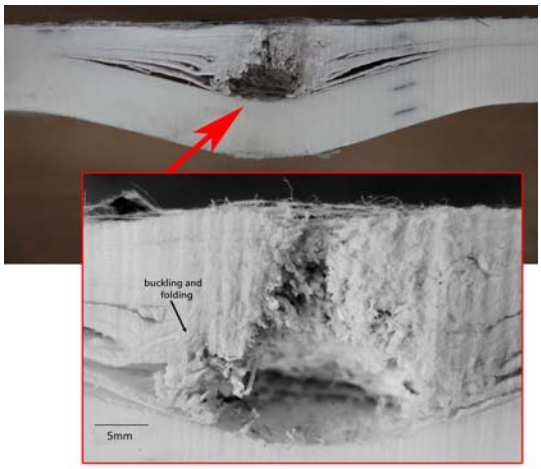

Figure 14: View at the impact point of the Dyneema HB26 panel.

impact event (typically substantially less, which was at the level of the measurement noise), regardless of the impact velocity. Unfortunately, it was impossible to conduct a similar analysis (the front face 3D DIC) on the Dyneema® panels.

4.4. Location of the First Major Delamination (FMD)

Figure 15 and Figure 16 present two full panels which were impacted at different velocities by two different projectiles. Typically during the ballistic trials, the rear part of a Dyneema® panel was drawn in during the projectile penetration. The kinetic energy of the projectile was dissipated by the lateral deformation of the rear part of the panel which acted as a membrane. As the material deformed out of plane, the edges of the rear part of the panel were drawn in, which created the substantial delamination, example of which is shown in Figure 15. A similar response was also observed for Spectra® 3124, however, the material appeared to be less stiff than Dyneema® which was pronounced by larger lateral deformations of the entire panel (including the front part of the panel), as shown in Figure 16. This large delamination is denoted in this paper as the First Major Delamination (FMD). Such nomenclature was implemented due to the fact that although, quite often, there were other smaller delaminations observed earlier, at the edges of the panel, there were always one or two larger ones, after which the deformation of the panel was different to what

Figure 15: Full Dyneema® HB26 panel impacted at 1410 m/s by a steel FSP.

Figure 16: Full Spectra® 3124 panel impacted at 466 m/s by a copper FSP.

was observed prior to this delamination (at the "front part" of the panel). It is noted also that the delaminations were apparent due to a relatively small panel size used for the trials. Most likely they would not be visible if 1 m^2 panels were used.

In order to estimate the exact location of the transition between the front part of the panel and the rear part of the panel (the part that experienced the membrane behaviour), the authors measured the distance from the front face of each tested panel to the first major delamination and plotted it against the striking velocity. Also, in the previous section it was noted that no movement of the front face material was observed for a short period of time, during each test with Spectra® panels. The author multiplied this time period by the striking velocity of the projectile in those tests in order to see at what depth of the panel the projectile was, when the front face surface movement was observed for a first time by the 3D DIC. This calulation was made for each Spectra® panel. All these measurements and calculations are presented in Figure 17 and Figure 18. The "0" value on the y-axis denotes the panel front face, the "24" value denotes panel rear face.

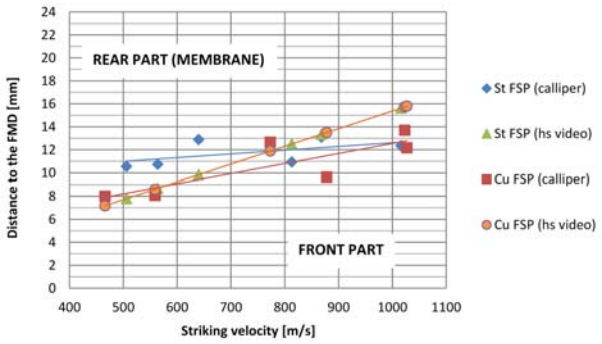

Figure 17: Location of the FMD for Spectra® 3124 panels.

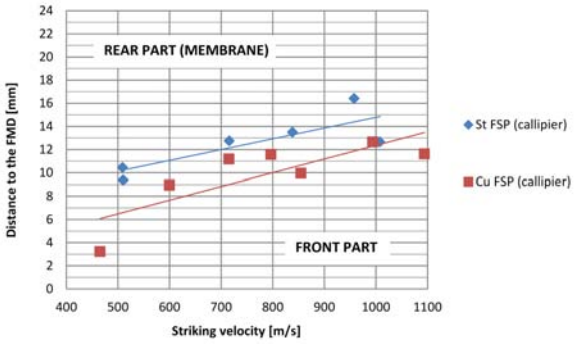

Figure 18: Location of the FMD for Dyneema® HB26 panels.

The presented data shows that the location of the transition region is striking velocity dependent. The first major delamination occurs deeper in the panel as the striking velocity rises. Also, the delamination occurred deeper in panels impacted with steel FSPs than in panels impacted with copper FSPs. However, it should be noted that the distance was measured using a calliper and the measured data was averaged over four sides of the panel. Thus, it is fair to presume that there is no (or there is very little) difference in the through thickness location of the transition plane, between the response of the two materials subjected to impact of steel and copper FSPs. Figure 17 shows that the distance obtained from the high speed videos is similar to the results obtained from the manual measurements. This indicates that there might be a relationship between the location of the FMD and the response of the front part of the material. It was noted in the previous section that the 3D DIC measurements revealed that the panels impacted at lower velocities tended to deform in-plane quicker than the panels impacted at higher velocities. Figure 17 shows that the panels impacted at lower velocities had also the front part of the panel thinner compared with panels impacted at higher velocities. Possibly, the deformation of the rear part of the material might have influenced the front face

deformation. A thinner front part would respond to the rear part deformation probably quicker. The slight difference in the curves slope (the manual measurements versus the high speed video measurements) might be the result of (on top of the measurement error discussed earlier) assumptions made on the timespan of the projectile presence in the front part of the panel - the limitation associated with camera frame rate (frame every 15.38 μs). This error could be reduced by using a higher specification camera (e.g. Phantom V2511) for the measurement.

In some cases, it was observed that at the rear surface of the front part of the panel the very outer layers experienced a very localized (approx. two projectile diameters) membrane-type of loading, which indicates that the transition region between the front part and the rear part of the panel, has a certain thickness i.e. it is not a sudden step change in the material behaviour. The latter ought to be confirmed by a fractographic analysis of the impacted panels and by Computed Tomography (CT) scans that will be conducted in near future.

4.5. The back face deformation

The experiments showed that the back face deformation of the panels differed substantially depending on the striking velocity. Figure 19 presents the out-of-plane deformation histories for the horizontal mid-plane section of the tested panels, obtained from the 3D DIC measurements. The plots were divided into three columns, from left: below the ballistic limit (except Spectra® 3124 impacted with steel FSPs), close to the ballistic limit, and at striking velocities substantially higher then the ballistic limit. The information about the striking velocity and the projectile type are provided in the top, left corner of each plot. The time frame stamp is provided next to each curve. The length of the plotted section was 220 mm, which is almost the entire length of the panel in the effective impact window. It should be noted that the sections used for the plot i), j), and k) were not in the mid-plane but slightly below, due to the poor speckle pattern in the mid-plane area. The authors understand that it might be more convenient to validate a numerical model using a one point time-displacement history. Thus, the time-displacement histories for a point located in the centre of the sections used for plots in Figure 19 are given in Figure 20 and Figure 21. The two charts are not further discussed herein as the focus is put on the data presented in Figure 19. It is observed that some of the curves are broken in Figure 19. This is a result of either panel damage due to the projectile penetration e.g. b), c), f); or due to problems with recognizing the pattern at high deformations e.g. a), i). The plots also show that not all shots were made exactly in the center of the panels e.g. c), g). A numerical artefact is also visible on the very bottom curve of the plot f) - the curve should be a smooth bump as all the other curves.

The data presented in the three columns of Figure 19 show that the response of the two materials changes with increase of the striking velocity. The materials response becomes more local as the striking velocity increases. The data shows that for the Dyneema® panels impacted below their BL (the first column), the initial deformation occurs at the impact point, in the in- and the out-of the plane directions, whereas at the final stages of the penetration, the out-of-plane deformation at the impact point does not change considerably while a substantial out-of-plane movement takes place at the areas remote to the impact point (see Figure 19d). It is noted that the deformation reaches the edges of the panel. This phenomenon is less pronounced for the Spectra® panels due to the fact that the panel, as mentioned previously, almost always split into two halves during projectile penetration. The 3D DIC measurements (plots h), i), and k)) shows that the unpenetrated Spectra® rear surface, at later stages of deformation, flew away towards the high speed cameras. The plots presenting deformation of panels subjected to shots at very high velocities (the third column) show that deformation of both materials is very local and the out-of-plane displacements are relatively low; less than 30 mm (except for the Spectra® 3124 impacted with steel FSP which split into two halves).

In general, the data in Figure 19 shows that Dyneema® HB26 was characterized by lower out-of-plane displacements than Spectra® 3124. Also, the deformation of Dyneema® HB26 impacted below or at the BL reached the edges of the panel (plots a), d), e) in Figure 19), while this was not taking place for the Spectra® panels impacted at similar striking velocities (plots g), h), j) and k)). This means that the load applied by the projectile was being distributed over the larger area in the Dyneema® case, compared with Spectra®. It appears that a similar size of area was being deformed for both materials, when impacted at very high velocities e.g. 1 km/s. These observations allowed to draw the following conclusions: a) most likely Dyneema® HB26 has higher interlaminar shear strength and shear stiffness than Spectra® 3124. The two properties allowed Dyneema® material to transfer the load applied by the projectile more effectively throughout the panel over the larger area, while deforming less than a comparative Spectra® 3124 panel.; b) the fact that deformation of both materials was similar at very high velocities while substantially different when impacted at lower velocities may indicate that the resin used as matrix system in both materials may be different (the

two may have different strain rate properties). The latter has a direct influence on how the applied load is transferred between the adjacent plies and within them. An alternative explanation is that as the matrix and the fibres are softened due to temperature rise caused by the shock, the projectile penetrates both panels in a similar manner. These generic conclusions are depicted by an example case presented in Figure 22.

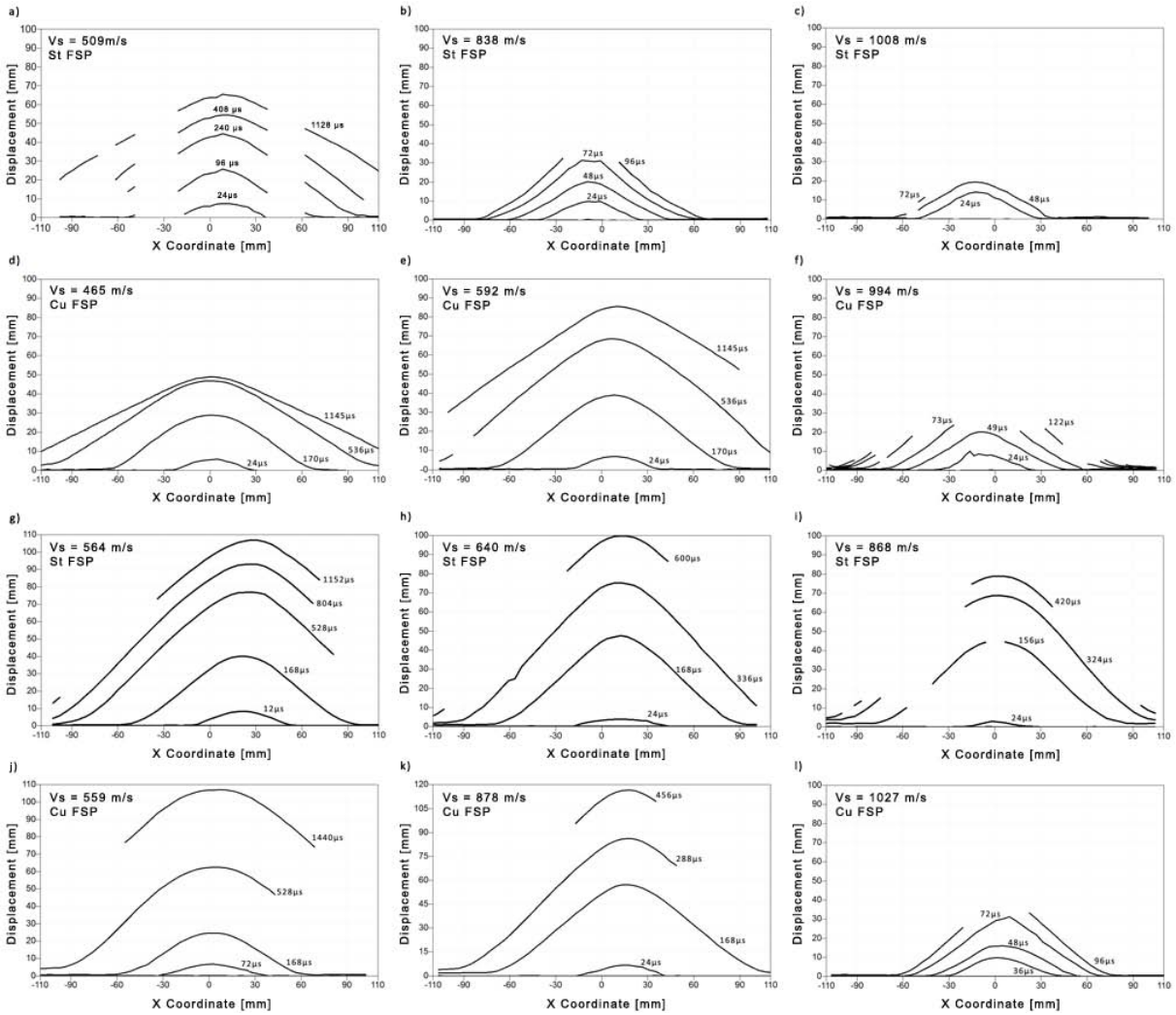

Figure 19: The out-of-plane displacement histories of the mid-plane horizontal section of the experimental panels, obtained from the 3D DIC measurements, for three different velocity ranges (below the BLs: a),d),g,j; at the BL or just above: b),e),h),k); substancially above the BLs: c),f),i),l)). Row 1: Dyneema HB26 impacted with steel FSP; Row 2: Dyneema HB26 impacted with copper FSP; Row 3: Spectra 3124 impacted with steel FSP; Row 4: Spectra 3124 impacted with copper FSP.

At 50 μs after the impact both Dyneema® and Spectra® panels seem to deform similarly in terms of the in-plane and the out-of-plane displacement. (The applied kinetic energy is probably dissipated by yarn straining, internal damage growth and the panel deformation. The in-plane waves propagate away from the impact point through the yarns). However, as the time progresses (120 μs) the in-plane deformation area of Spectra® increases only to a small extent, most of deformation takes place out of the plane; while the deformed in-plane area of Dyneema® increased in size about twice. The out-of-plane panel deformation also increased. (Most likely the low shear strength of Spectra® allowed for quick delamination growth in one or more planes inside the panel thus allowing for less restricted out-of-plane movement. The higher shear strength and shear stiffness of Dyneema®, possibly in conjunction with the influence of the material layup, facilitates further in-plane load transfer. The waves continue to propagate towards the

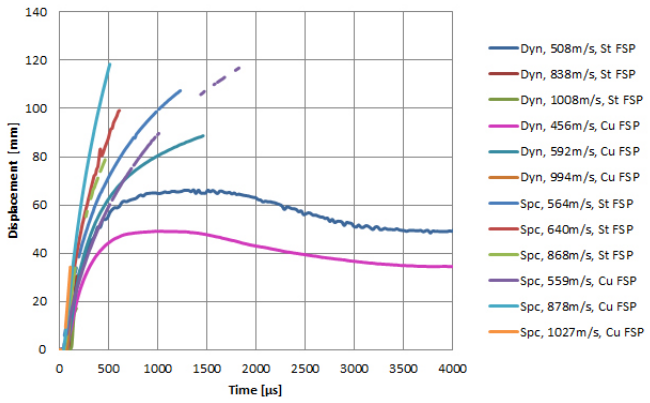

Figure 20: Time-displacement history of the point on the rear surface of the tested panels.

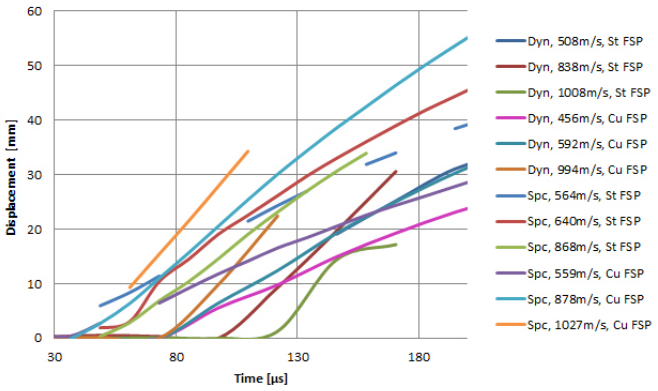

Figure 21: Time-displacement history of the point on the rear surface of the tested panels - magnified view.

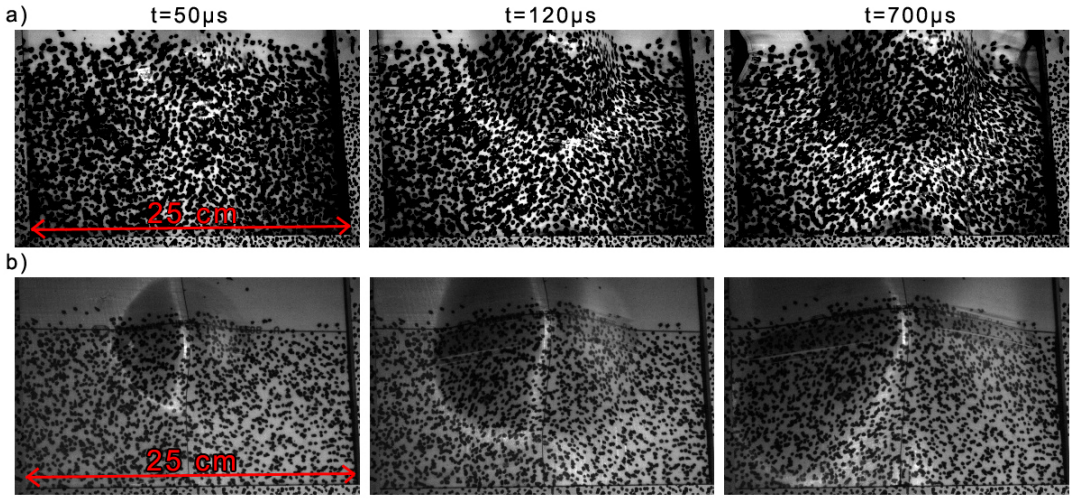

Figure 22: Comparison of the back face deformation of two panels impacted at approximately 510 m/s with steel FSPs: a) Spectra® 3124; b) Dyneema® HB26.

edges of the panel. The initial circular deformation shape becomes a rectangle as the load is transferred via shear in the regions between the primary yarns perpendicular to each other. It is emphasized that the above statements on the shear strength and stiffness of the two materials are entirely based on the shear deformation information obtained from the DIC measurements, which are described in the subsequent section). During the following 580 μs the tensile wave travelling in the mid-plane of Spectra® panel reached the edges of the panel, which was pronounced as the drawing-in of the primary fibres. In terms of Dyneema® the in-plane deformation reached the edges of the panel, while the out-of-plane deformation further increased. No drawing-in was observed. (Possibly the low intralaminar shear strength of Spectra®, or extensive slippage at the yarn/matrix interface, or ductility of the used matrix, or all of these together allow for extensive in-plane movement of the primary and the secondary yarns, as the out-of-plane deformation progresses). In the subsequent deformation stages (not shown in here) the Dyneema® captured the projectile and ”relaxed”, while the the Spectra® also captured the projectile, but the rear part of it almost completely slipped out of the rig. The latter is believed to be associated with the edge effects. It is noted here that when determining the ballistic limit of a composite panel the edge or boundary of the panel should not affect the result, otherwise the ballistic limit is determined for the specific panel size, and may not be a function of its thickness. A common assumption is that the transverse or kink wave speed does not reach the boundary and return to the impact site during the event, i.e. during penetration of the

panel, which typical occurs in less than 200 microsecs. For UHMWPE and the velocities considered in this paper the boundary or edge support conditions should not affect the ballistic limit results.

Figure 23 presents strain readings from the same section that was used in Figure 19. Each plot in the figure shows the highest strains recorded in a number of time frames - this should give the reader an appreciation of what strains the panels experienced throughout the experiments. The logarithmic strain in the horizontal direction, denoted as *Epsilon X*, is plotted on the Y-axis (0.04 is the maximum value on each chart). All other annotations remain the same as in

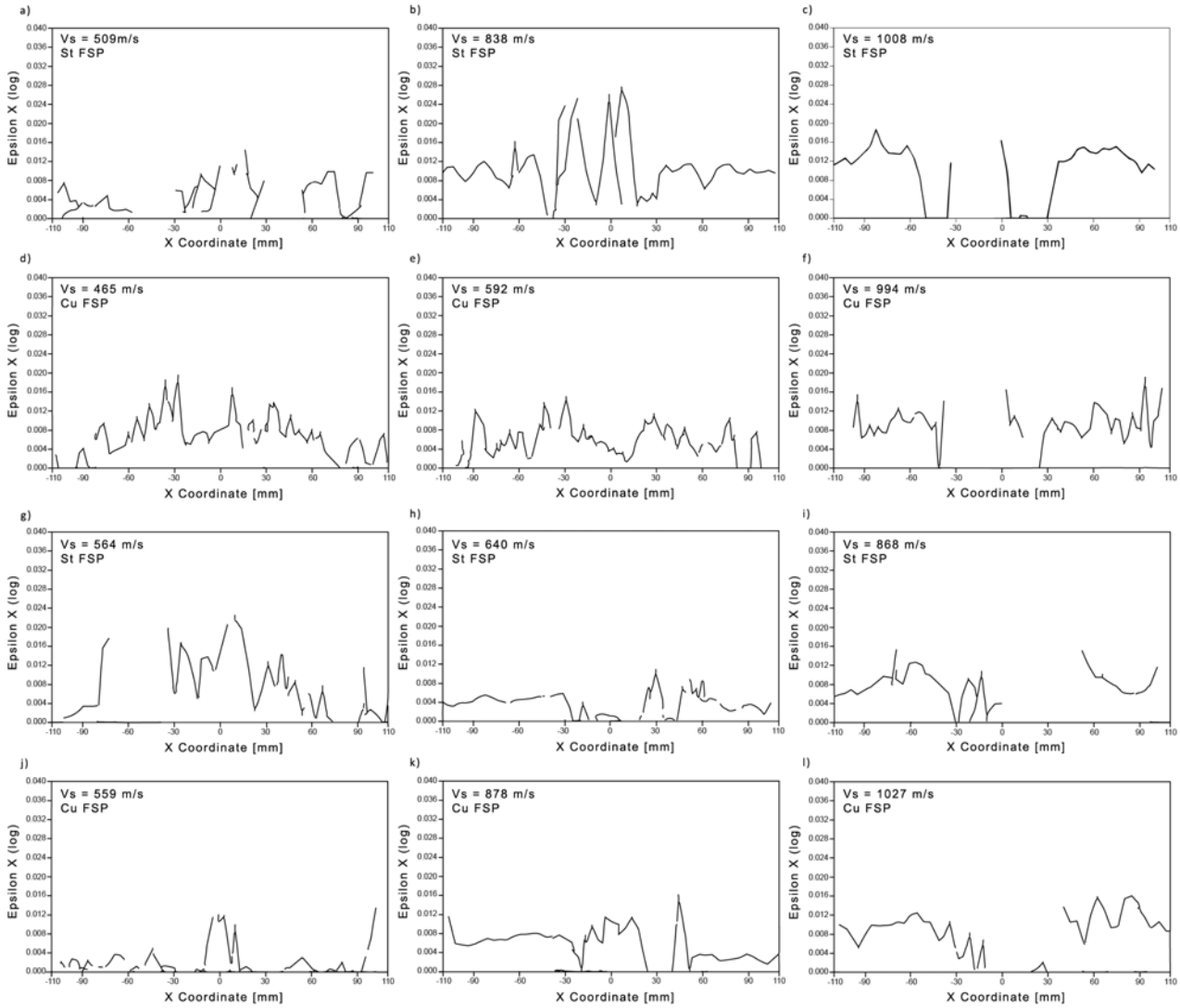

Figure 23: The in-plane strain histories of the mid-plane horizontal section of the experimental panels, obtained from the 3D DIC measurements, for three different velocity ranges (below the BLs: a),d),g),j); at the BL or just above: b),e),h),k); substancially above the BLs: c),f),i),l)). Row 1: Dyneema HB26 impacted with steel FSP; Row 2: Dyneema HB26 impacted with copper FSP; Row 3: Spectra 3124 impacted with steel FSP; Row 4: Spectra 3124 impacted with copper FSP.

Figure 19. Although the charts look "noisy", it is not noise that is presented but the actual data from many time frames overlaid on each other. The spikes are partially a result of relatively low camera frame rate that was used. The curves would be more smooth, if a higher camera frame rate was used (which was impossible during the experiments due to the selected resolution). It is observed that as the striking velocity rises (from the first column on the left to the third column), the fewer readings were plotted. This is due to the fact that as the measurement setup remained the same throughout all experiments (cameras resolution and frame rate) but the striking velocity increased, the material

penetration occurred faster, hence fewer frames with the readings. It should be also emphasized that in many cases due to the destructive nature of the experiment it was possible to record only one or two frames at the very impact point before the pattern was damaged and no DIC measurements were made.

The data shows that regardless of the striking velocity the primary yarns and the secondary yarns at the back face of the panels experienced strains of no more than 2% throughout most of the measured length (mind the caveats mentioned above). By using the interpolation tool provided in the DIC software, it was possible to get an estimate of what strains would the panel experience at the very impact point just before the failure, based on the data from the adjacent regions. For plots a), d), e), and g) no interpolation was needed as the panels were not penetrated and the row data was of good quality. In cases b), c), and f) the interpolated data showed (not presented in here) that the Dyneema® primary yarns experienced about 6% strain at the very impact point, for a very short period of time, prior to failure. Interpolated plots h) and k) showed that the Spectra® primary yarns experienced about 4% elongation at the impact point. It was impossible to extract any additional data from cases i) and l) as the raw data was not sufficient for the analysis. These interpolated values should be treated with caution as they are purely the effect of a numerical interpolation. However, the values do not seem extremely unrealistic as it is possible that during the penetration the shock heating could have caused thermal softening of the yarns in the membrane region as well. This would relax the transverse molecular bonds (van der Waals and the chain entanglement) between the aligned polyethylene chains and thus allow for slipping of the molecules on each other. The latter would be perceived on the macro scale (the DIC) as an excessive straining. If the hypothesis is true, this would mean also that the fibres would also not reach its statically determined (tensile tests on yarns) Ultimate Tensile Strength, but would fail at some lower value of stress. Another explanation of the phenomena is that although the DIC system would measure the yarn stretch during the impact event, it has been observed that during static and dynamic testing of the yarn failure of the individual fibres occurs throughout its length, rather than localising at a specific yarn failure site. Hence the DIC system may be interpreting the multiple fibre failure as an increase in the length of the yarn, as the strain in the fibre is not directly measured due to the scale of the DIC pattern. Nevertheless, it is also possible that the fibres at the back face were sheared or pulled to fracture by the projectile, which would mean that the discussed interpolated values are incorrect. A detailed fractographic work is required to identify the actual mode of failure of the fibres located at the rear face of the tested panels.

It appears that both steel and copper FSPs apply similar strains to the panels. By comparing the strains experienced by the panels with their deformation (see Figure 19), it was observed that regardless of the extent of panel deformation, the maximum experienced throughout the panels strains were similar (this statement excludes the data obtained from the interpolation i.e. the presumed very high, localized strain values at the impact point). This implies that large material lateral deformations do not necessarily mean higher yarn straining (which is believed to be one of the main energy dissipating mechanisms) i.e. the large material lateral deformations do not necessarily mean better ballistic performance. The analysis of strain-time history in the panels rear surface showed that the primary yarns experienced the highest strains throughout all their length immediately after the flash generated at the front face vanished (the flash was also visible at the back face although the panels were not transparent), which was recorded to take place within 25 μs and 12 μs after the flash, for Dyneema® HB26 and Spectra® 3124 respectively (different camera frame rate was used). In the subsequent time frames the strain quickly dropped to zero (within approx. 50 μs) in the regions remote to the impact point. It appears that the rate of decrease of the strain values in the impact region in Dyneema® was striking velocity dependent. The amount of strain in the panels impacted at low velocities (the first column of Figure 23) seemed to gradually decrease as the panel continued to deform laterally. The rate of decrease of the strain values was much higher in Dyneema® panels impacted at higher velocities. In terms of Spectra® 3124, it was observed that the entire length of the primary yarns unloaded very quickly and although the material continued to experience large lateral deformations the yarns were not strained (nearly no strain at the tip of the impact cone for shots that resulted in panel splitting). It is believed that this observation points out again at the shear properties of the material. Possibly, although the yarns experienced the maximum strains at the initial stages of the penetration, the matrix system and the fibre/matrix interface did not facilitate transferring the load further. The material quickly delaminated and hence there was nothing constraining the two parts of the panel which could guarantee load transfer to further areas of the material.

The described difference in the materials behaviour is also visible in the post-mortem panels. Figure 24 and Figure 25 show damaged Dyneema® HB26 and Spectra® 3124 panels. It was observed that Dyneema® panels delaminated in a more catastrophic manner (the fibres were torn away from the plies), while Spectra® panel had relatively "clean"

surfaces (almost no tearing or debonding of fibres).

Figure 24: Full Dyneema® HB26 panel impacted at 609 m/s with a steel FSP.

Figure 25: Full Spectra 3124 panel impacted at 640 m/s with a steel FSP (the two split parts being held together by the author).

4.6. The in-plane shear behaviour

The observations and conclusions given in the previous section were also confirmed by the measurement of shear deformation at the back face of the panels. Figure 26 shows an example digital mesh obtained from the 3D DIC measurements with the diagonal section used for extraction of data on shear deformation. The figure shows also the mid-plane section that was used for plotting data in Figure 19 and Figure 23. Figure 27 shows in-plane shear time histories for the Dyneema® and the Spectra® panels. The in-plane shear is denoted as *Epsilon XY* on the Y-axis, while the time steps are give next to the curves.

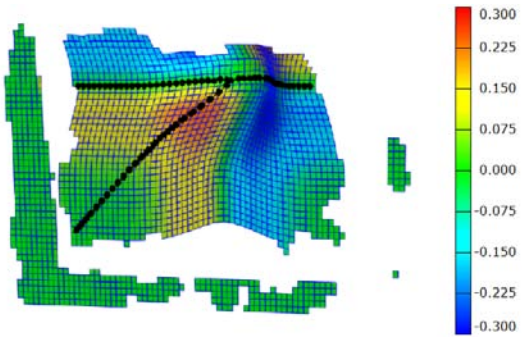

Figure 26: Digital mesh of deformed Spectra® 3124 impacted at 640 m/s by a copper FSP (in-plane shear plotted).

The data plotted in the Figure 27 indicates that there were substantial shear deformation taking place during the impact events. As expected, very little or no shear deformation was present at the impact point (“0” value on the X-axis), where the primary yarns were expected to dissipate the projectile kinetic energy by straining. The largest extent of shear deformations in Dyneema® HB26 panels, during the period when the panel had not been penetrated yet, took place when the striking velocity was below or at the BL of the material (charts a), d) and e) in Figure 27). At these velocities the in-plane shear deformation quite often reached the boundaries of the panels, while the peak value of the in-plane shear deformation during the impact event reached up to 20-25%. This supports the description of the Dyneema® deformation that was presented in the previous section. It was observed also that there was a residual in-plane shear deformation in the panels that were not penetrated, which levelled out itself, as the panel was ”relaxing” after the impact, to a value of 5-10% (see charts a) and d) in Figure 27). The peak in-plane shear

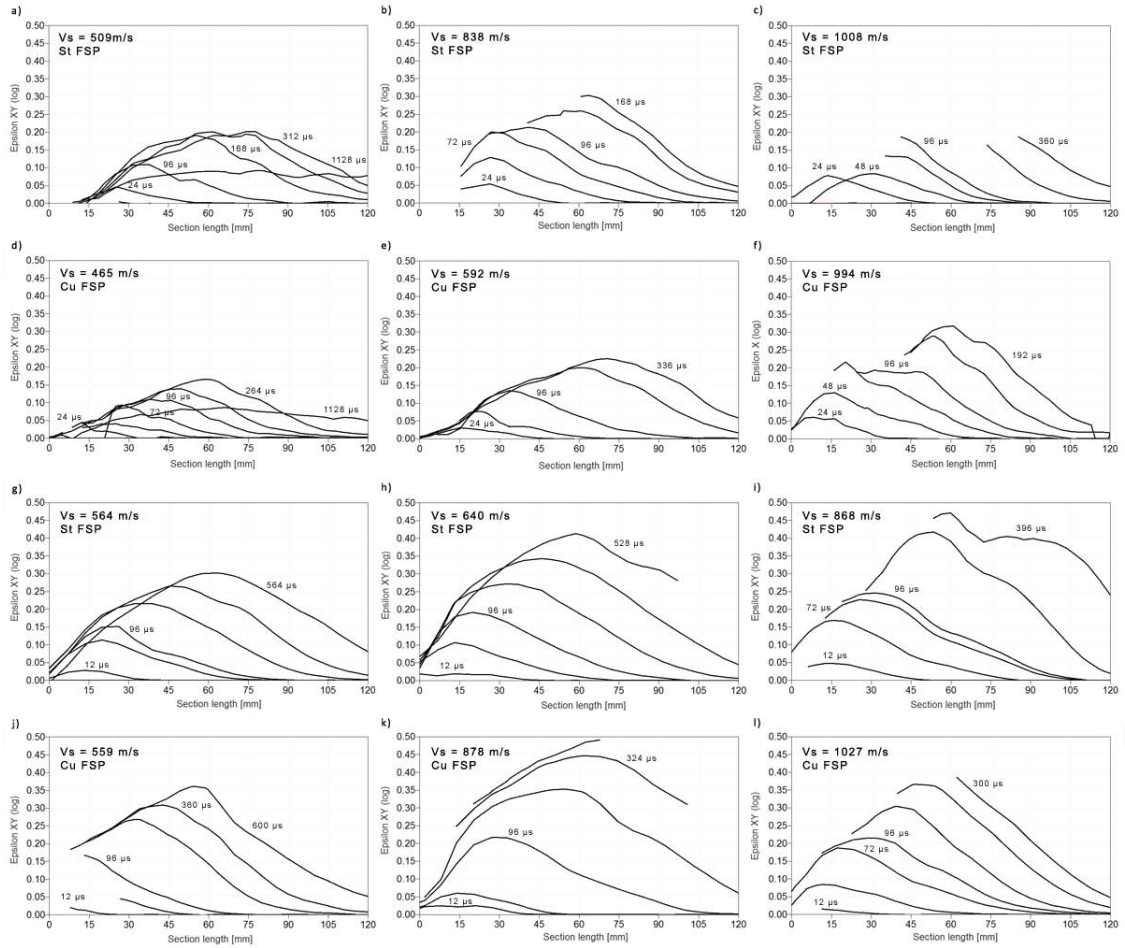

Figure 27: In-plane shear strain histories of the diagonal section of the experimental panels from the 3D DIC measurements, for three different velocity ranges (below the BLs: a),d),g,j; at the BL or just above: b),e),h),k); substancially above the BLs: c),f),i),l)). Row 1: Dyneema® HB26 impacted with steel FSP; Row 2: Dyneema® HB26 impacted with copper FSP; Row 3: Spectra® 3124 impacted with steel FSP; Row 4: Spectra® 3124 impacted with copper FSP.

value seemed to decrease with increase of the striking velocity. In the experiments where Dyneema® was impacted at approx. 1 km/s the peak value was 10-15%, before the projectile penetrated the panel (see charts c) and f) in Figure 27). Spectra® 3124 experienced far higher in-plane shear deformations than Dyneema® HB26. The peak in-plane shear values for Spectra® panels impacted at 500-600 m/s ranged from 30 to 35%. The peak in-plane shear values, before the penetration, for the two shots fired at 868 m/s and 1027 m/s were 18% and 23%, respectively; which is about a double of the Dyneema® values for similar shots. At these velocities Dyneema® panels failed within 48 μs while Spectra® panels within 72 μs. It was observed that at these high velocities the shear deformation of Dyneema®, before penetration, was enclosed within approx. 65 mm radius from the impact point, while the extent of shear deformation of Spectra® reached about 100 mm radius. Also, it appears that steel projectiles left a different in-plane shear deformation "signature" than the copper projectiles. Charts a), d), g), and j) in Figure 27 show that the shear strain time history over the measured section had a dome shape for steel projectiles, while being more triangular for panels impacted with copper projectiles. This is probably related to the fact that the copper FSPs were more prone to plastically deform, due to their low yield strength and the adiabatic heating previously described, compared to steel projectiles.

5. Conclusion

The presented study compared the ballistic behaviour of Dyneema® HB26 and Spectra® 3124 subjected to impact of 20 mm diameter copper and steel Fragment Simulating Projectiles, fired in the 400 - 1000 m/s striking velocity range. The highly instrumented, state-of-the-art experimental setup allowed to extract vast amounts of data on the materials behaviour during the projectile penetration, required for validation of advanced numerical models.

The results showed that Dyneema® HB26 had slightly higher ballistic limits than the latter, nevertheless, the response of the panels was most likely affected by the edge effects, as a relatively small, with respect to the applied loads, panel size was used. It is possible that the larger panels would show different ballistic limits of the materials. Also, for precise determination of the ballistic limit, more panels should be tested.

It was observed that at very high striking velocities (850 m/s and above) both materials had very similar ballistic performance. The steel projectiles deformed very little during the impact and this only took place at firings at 1 km/s or above. The deformation of the copper FSPs increased with increasing striking velocity. The observed deformation, however, was a result of the impact on both the tested panel and the catcher box used in the study. The influence of the latter could be minimized, if an alternative to sand was found/used e.g. gelatine, however the cost of such solution would probably be much higher. In general, the panels lost very little of their initial mass due to impact (less than 1%). It was observed that the panels impacted with copper FSPs lost more weight than panels impacted with steel FSPs.

The front 3D DIC measurements allowed identifying how the front face of the panels deformed in-plane and out-of-plane in time. It was observed that the in-plane movement of the material occurred first, before the out-of-plane movement. Although the projectile material did not influence the in-plane response of the panels, the out-of-plane response was affected. The measurements showed also that the front face of the Spectra panels experienced less than 1% tensile straining during the projectile penetration.

A post-mortem observation of the test panels showed that the deformation characteristics of each panel changed in the through thickness direction. It was observed that at a certain distance away from the front face a large delamination(s), which reached to the edges of the panel, occurred, after which the remaining part of the panel was drawn in. By plotting the location of this delamination (denoted as the First Major Delamination) against the striking velocity, it was identified that the through thickness location of the FMD was striking velocity dependent. It occurred further away from the impact face as the striking velocity rose.

The 3D DIC measurements of the rear part of the panel, which acted as a membrane during penetration, allowed analysis of the back face deformation characteristics of the two tested materials. It was observed that the response of the materials changed (became more local) with increase of the striking velocity. The measurements showed that the primary and the secondary yarns at the back surface experienced not more than 2% strain, independently of the striking velocity, at the areas which were not a direct point of exit of the projectile. The interpolated data at the point of the projectile exit (which was not possible to measure during the experiments) indicated that the strains in this region might have been as high as 6%. Nevertheless, the accuracy of this interpolation remains to be investigated. The in-plane shear behaviour was found to be very different for the two tested materials. Spectra® panels experienced about twice higher shear deformations than comparable Dyneema® panels. It was observed that there was a residual shear deformation in Dyneema® panels impacted at low velocities, at the level of 5-10% of shear strain. The measurements showed also that the panels impacted with steel projectiles had different in-plane shear deformation than panels impacted with copper projectiles.

Overall, it was observed that the large out-of-plane deformations of the panel rear part are not an indicator of a better ballistic performance, but rather of a lack of optimization of the interlaminar and intralaminar shear properties of the material. The findings indicated that the dynamic in-plane shear behaviour plays a crucial role in the ballistic performance of a unidirectional cross-ply, high performance composite materials.

Although the paper provided an in-depth insight into the ballistic behaviour of the two high performance composite materials, it was impossible to directly prove some of the statements made by the authors. Therefore, the future work will involve fractographic work and computer tomography scans of the tested panels, that should identify validity of the statements. As 3D Digital Image Correlation becomes more frequently applied to various dynamic experiments, it seems prerequisite to identify the accuracy of the strain measurements provided by commercial DIC systems.

Acknowledgement

The authors would like to acknowledge funding from the EPSRC and the Dstl grant EP/G042861/1. The research would not be possible without support from Vision Research UK represented by Mr Jolyon Cleaves. The support of DSM, that provided Dyneema® HB26 for the study, is greatly appreciated. Special thanks to Dr Ian Softley from DSTL, and to Dr Adam Connolly, Dr Stefano Del Rosso, Mr Joseph Meggyesi, Dr Lucio Raimondo, and Michelle Willows from Imperial College London for help during the trials.

References

[1] Cheeseman, B. A., *Ballistic impact into fabric and compliant composite laminates*. Composite structures,2003,Vol. 61, p. 161-173.

[2] Iremonger, M. J., Went, A.C, *Ballistic impact of fibre composite armours by fragment-simulating projectiles.* composites Part A, Vol.26A, p.575-581.

[3] Prosser, R. A., *Penetration of nylon Ballistic Panels by Fragment-Simulating Projectiles. Part I: A linear approximation of the relationship between the square of the V_50 or V_c striking velocity and the number of layers of cloth in the ballistic panel.* Textile Research Journal,1988, Vol.58(3), p.161-165.

[4] Prosser, R. A., *Penetration of nylon Ballistic Panels by Fragment-Simulating Projectiles. Part II: Mechanism of penetration.* Textile Research Journal,1988, Vol.58(3), p.61-68.

[5] Figucia, F., Williams, C., Kirkwood, B., Koza, W., *Mechanisms of Improved Ballistic Fabric Performance.* 1982. Technical Report, U.S. Army Natick Research & Development Center

[6] Scott, B.R., *The penetration of compliant laminates by compact projectiles*. In: Proceedings of the 18th International Symposium on Ballistics. San Antonio, Texas, 15-19 November 1999. p. 1184-91.

[7] Lee, B. L., Walsh, T. F., Won, S. T., Patts, H. M., Song, J. W., Mayer, A. H.,*Penetration Failure Mechanisms of Armor-Grade Fiber Composites under Impact.* Journal of Composite Materials, Vol. 35, No. 18/2001.

[8] Flanagan, M. P., Zikary, M. A., Wall, J.W., El-Shiekh, A., *An experimental investigation of high velocity impact and penetration failure modes in textile composites.* Journal of Composite Materials, Vol. 33, No. 12/1999.

[9] Cunniff P. M., *Dimensionless parameters for optimization of textile-based body armor systems*. In: Proceedings of the 18th International Symposium on Ballistics, San Antonio, Texas, 1519 November 1999. p. 130310.

[10] STANAG 2920 Edition 2 Ballistic Test Method for personal armour materials and combat clothing; July 2003.

[11] Greenhalgh, E. S., Bloodworth, V. M., Iannucci, L., Pope, D., *Fractographic observations on Dyneema composites under ballistic impact.* Composites: Part A. 2012.

[12] Hazell, P. J., Appleby-Thomas, G. J., Trinquant, X.,Chapman D. J. *In-fiber shock propagation in Dyneema*. Journal of Applied Physics, 2011, Vol. 110.

[13] DSM product data sheet: Dyneema SK76 dtex1760 TZ25. 2006

[14] Qi, H.J., and Boyce, M.C. *Stress - strain behavior of thermoplastic polyurethanes*. Mechanics of Materials, 2005, Vol. 37, p.817-839.